



## “STARAYA PODSTANCIYA” LANDSLIDE AND GEOPHYSICS

### SESUV “STARAJA PODSTANCIJA” A GEOFYZIKA

*Pavel Bláha<sup>1</sup>, Shavkat Abdullaev<sup>2</sup>, Igor Motornyj<sup>2</sup>, Rustam Niyazov<sup>2</sup>, Milan Lazecky<sup>3</sup>, Jan Gebauer<sup>1</sup>*

#### **Abstract**

This paper wishes to show the cooperation of specialists of both countries, which is recently taking place unofficially without any grants on both parties with a few exceptions, on the example of the Staraya Podstanciya landslide close to the town of Angren in Uzbekistan. This system of cooperation fully developed at the time of practical halting of conventional methods of communication. By transition to the electronic communication of the system of remote conferences, it is possible to reliably communicate without national or international grants. In this paper we wish to show possibilities of using geophysics in the survey of extensive slope failures with very rapid movement. The volume of the studied slope failure is 120 million cubic metres (120 Mm<sup>3</sup>) and its maximum measured velocity was 750 millimetres per day.

#### **Abstrakt**

Tento článek chce na příkladu sesuvu Staraja Podstancija v blízkosti města Angren v Uzbekistánu ukázat spolupráci specialistů obou zemí, která v poslední době až na výjimky probíhá neoficiálně bez jakýchkoli dotací na obou stranách. Tento systém spolupráce se plně rozvinul v době praktického zastavení klasických způsobů komunikace. Přejdem na elektronickou komunikaci systému dálkových konferencí, lze spolehlivě komunikovat, bez jakýchkoli dotací, ať již národních nebo mezinárodních. V tomto příspěvku chceme ukázat možnosti použití geofyziky při průzkumu rozsáhlých svahových deformací s velmi rychlým pohybem. Objem studované svahové deformace je 120 milionů kubických metrů (120 Mm<sup>3</sup>) a jeho maximální naměřená rychlost byla 750 milimetrů za den.

#### **Keywords**

*Electrical resistivity tomography, seismic tomography, radar interferometry, temperature, resistivity profiling, electrical resistivity sounding*

## Klíčová slova

*Elektrická odporová tomografie, seismická tomografie, radarová interferometrie, teplota, odporové profilování, vertikální elektrické sondování*

## 1. Introduction

The Staraya Podstanciya (SP) slope failure lies on the northern mining wall of a bituminous coal pit close to the town of Angren. Since the early 1980s, new enormous landslide began to appear on the walls of the giant opencast pit. The length of the SP landslide at the beginning of its existence was 750 m, its volume being 58 million cubic metres ( $\text{Mm}^3$ ) and the velocity of movement being 20–24 mm/day. The dimensions of the landslide changed not only by its own movement, but also by mining activity, due to which its toe was excavated. Around the year 2010, the landslide expanded and absorbed also minor surrounding landslides. In that year, the length of the scarp crack reached a value of 1400 m; at that time, the landslide was 900 m long and had an average thickness of 100 m. After the initial great velocity of movement, its velocity gradually decreased from 750 to 45 mm/day and the overall movement per the year 2011 reached 100 m horizontally with a vertical drop of 50 metres. The today's state of the slope failure is well visible from a satellite image dated 5 May 2023 (Fig. 1).

In addition to the conventional engineering-geological and geodetic methods, the landslide was also monitored geophysically. Besides new measurements, archival geophysical measurements were also used to describe the rock mass around the landslide, particularly vertical electrical sounding (VES) carried out eight years ago with the task to contribute to the knowledge of the geological structure of the rock mass in conjunction with the monitoring of the state of groundwater. Three profiles were newly measured using electrical resistivity tomography (ERT), shallow seismic refraction (SSR), ground-based seismic tomography and thermic profiling. ERT measurement was used to obtain curves of electrical resistivity profiling and curves of vertical electrical sounding by transforming the output tables. The field outputs of ERT were evaluated in Tashkent using the ZondRes2D program and the Danish RES2DINV program at the Geotest workplace. After the evaluation of individual measurements, both old and new, we proceeded to the combined geological-geophysical interpretation. With the use of such two programs, we have good experience which bring particularly the possibility of finding out which variations of the resulting resistivity fields can be expected (Bláha et al., 2021, Tábořík et al., 2017).



**Fig. 1** Satellite image of the landslide dated 2 May 2023

## 2. Geology and archival measurements

The geological structure of the site is represented by a layer of Quaternary gravels (up to 70 m thick), Palaeogene silty sands, plastic clays and sandstones (up to 35 m thick), Neogene clays, sandy marlstones and limestones (up to 30 m thick). Kaolin clays, siltstones and sandstones are 25 m or less thick, while the coal production layer is up to 70 m thick. Landslides occur in the contact zone of the Alai limestones with sandstones and clays of Suzak sediments. The Alai Stage is represented by limestones 10–30 m thick, stiff, with porosity 15.8% and strength 20.7 MPa. The rocks have low water content (3.4 %). They are not water-absorbing and are relatively stable and moderately weathered. The Suzak Stage, 10–40 m thick, is composed of sandstones, gravel clays and conglomerates with sandy-marly clays. The hydrogeological conditions in the Angren coal pit are distinguished by four water-bearing bodies: Quaternary, Cretaceous-Palaeogene, Jurassic and Palaeozoic. The rock mass is fed by atmospheric precipitation, surface runoff from wadis and infiltration through tectonic zones.

The intensity of waterlogging of rocks and the occurrence of groundwater lead to the relatively broad development of landslide processes. The possibility of drainage of layers is determined by the fact that the depression curve has a steep character and lies in the intermediate proximity to the surface of the pit wall.

In 2015, north of the bituminous coal pit, two profiles of VES (PIV and PV) were measured. The profiles were located about 200 and 460 metres, respectively, north of the scarp edge of the SP landslide. The profiles were up to 0.9 and 6.1 km long, respectively, and their purpose was to assess the structure of the rock mass and to find places of decreased resistivity, which could be accompanied by higher water saturation (Niyazov et al., 2020). It is not a surprise that these investigations used conventional measurement and evaluation. Figure 2 shows an example of the graphic output of these measurements from a part of profile PV. Four types of Quaternary soils and one collective type of rocks of the basement were identified from the quantitative evaluation by the size of resistivity. The authors of the then report did not make any trial how to differentiate the rocks of the pre-Quaternary. In addition to this quantitative evaluation, the contours of apparent resistivity

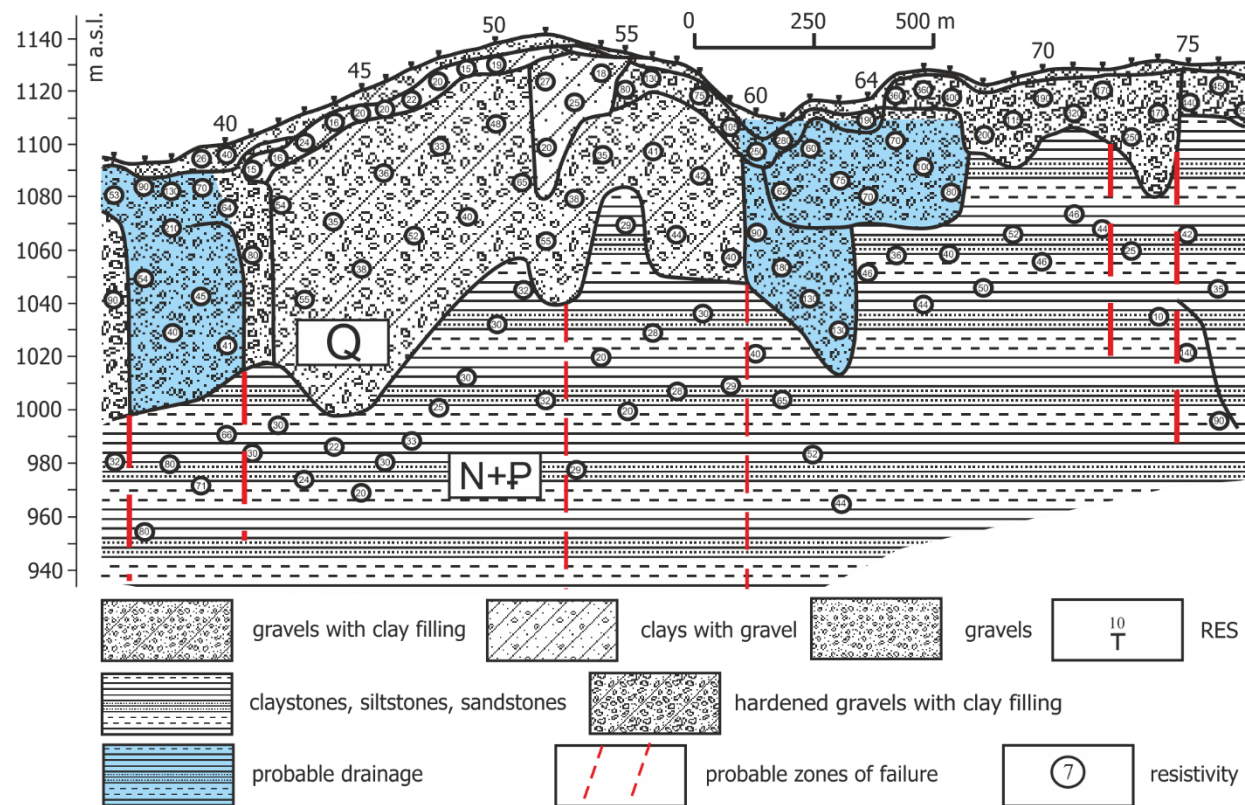


*Fig. 2 An example of archival interpretation of VES*

were constructed on all profiles in cross-sections. We used them in engineering-geological interpretation to search for preferred pathways of groundwater.

### 3. Measurements carried out in the year 2019

The results of this stage of measurement were processed by the Uzbek party in two forms at the first stage. The first included graphs of thermic measurements and the second was geophysical cross-sections using subsurface exploration methods on all three profiles.

As already mentioned, new measurement comprises measurement on three profiles using four methods (Fig. 3). At the same time, it is necessary to say that not all of these methods were applied on all profiles. Thermic profiling was measured on two profiles P1 and P3 contactless using the OMEGA apparatus of the OS530HRE type. The interval of thermic measurements was 10 m and measurement was conducted as follows: on 7 July 2019 between 4.35 and 5:15 on P1 and on 5 July 2019 between 4:48 and 5:37 on P3. The results of measurement are given in Figure 4, in which thermic profile P1 is marked in red and profile P3 in green. The results of measurement are rather interesting in relation to the methodology of measurement. All data on the measurement are given in the figure. The measurements were carried out just after the sunrise, but at the time of measurement there was still a shadow on the measured profiles. The temperature of air before and after the measurement was not read out. The temperature along the profile changed by up to 4°C. Why, however, the temperatures differ so much on the profiles is not clear. The error of measurement was not determined; the only place in which it is possible to estimate the error of measurement is the crossing of profiles where the temperature differs by 0.6°C from one another. Both the profiles lie on the body of the landslide, and so it is surprising that

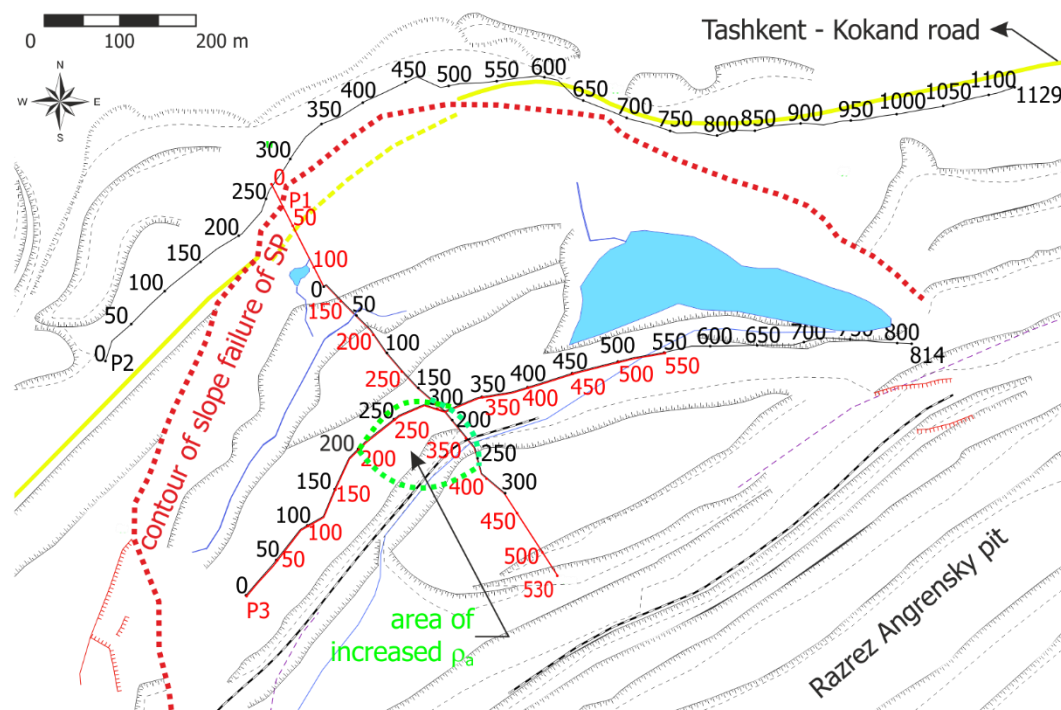


Fig. 3 Layout plan of geophysical profiles on the SP landslide

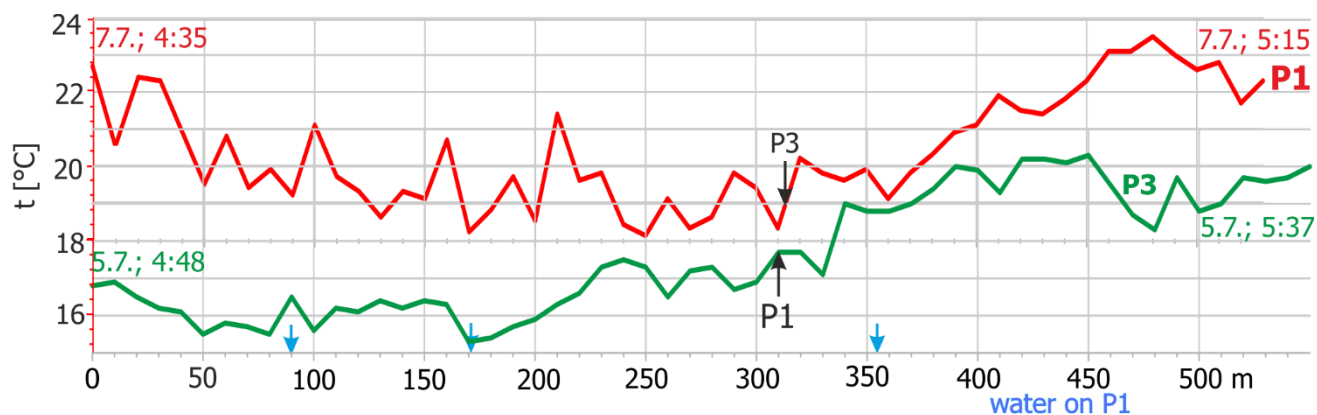
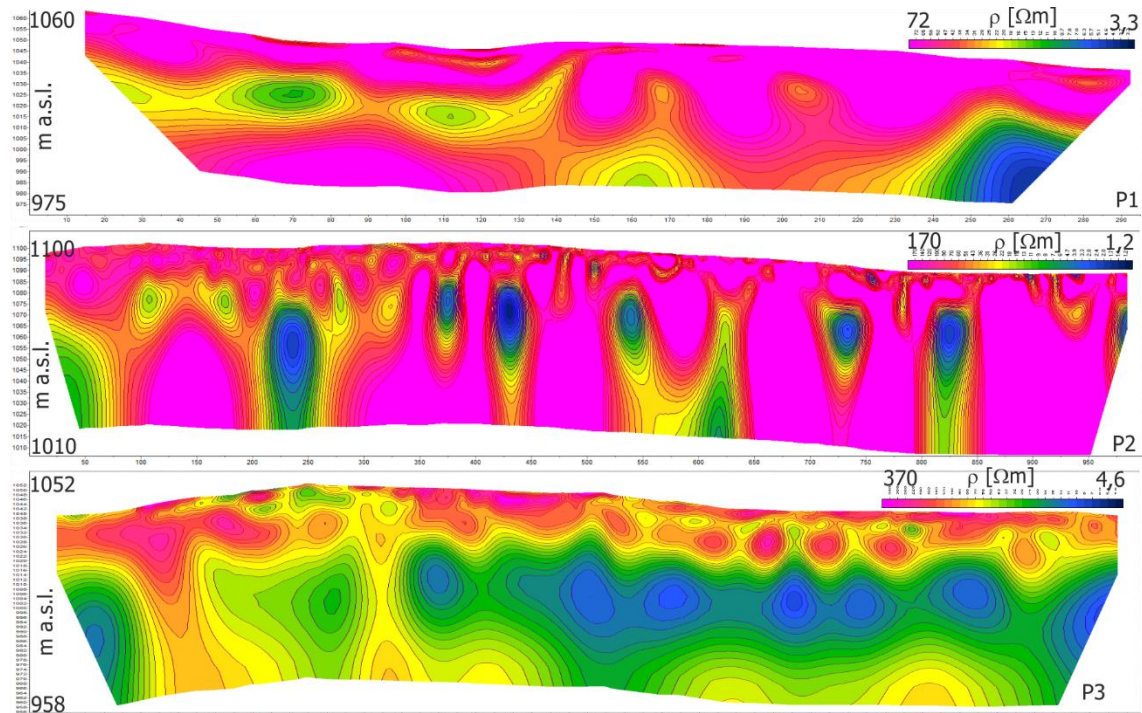


Fig. 4 Results of thermic measurements

the temperature between the beginnings of the profiles differ by up to about 5.5°C. In the middle part of the profiles, the temperatures on both the profiles come near to about 1°C. At the end of the profiles, the temperatures again differ, namely by up to five degrees. According the map of landslide and a field traverse, it is not possible to find an explanation for this fact. Similarly surprising was that no anomalies were recorded in the places of movement of water on landslides.

Electrical resistivity tomography was measured between 20 and 22 July 2019 on all three profiles with an interval of 5 metres, except the first and last 100 m where the interval of measurement was 10 m (Fig. 5). The basic length of array was 400 m; in case of need, the section of 200 m of the first array was always overlapped by another section. Measurement was carried out using the Swedish apparatus Terrameter LS (Abdullaev et al., 2020). Measurement was evaluated by the Moscow program ZondRes2D. ERT was measured in the Wenner–Schlumberger system and profile P1 also in the dipole–dipole system (Fig. 6). When viewing three cross-sections of ERT, three questions arise. The first is whether it is advantageous to plot the field of resistivity values in each profile in the same size of depths. Profile P1 comes out even “underexaggerated”, namely about twice, i.e. 100 m in the direction of the axis x is twice longer than in the direction of the axis y, which is quite an unusual solution. Profile P2 is exaggerated 1.8 times and profile P3 1.35 times. It seems that it would be more suitable to depict profiles on the same scales. The second question is the choice about to what depth to depict the fields of resistivity values. If it is suitable to use the conventional AB/2, or to choose the depicted depth smaller, i.e. AB/4 or even AB/5. When choosing the same scales, it is possible to characterise better the differences between the



**Fig. 5** Original results of electrical resistivity tomography

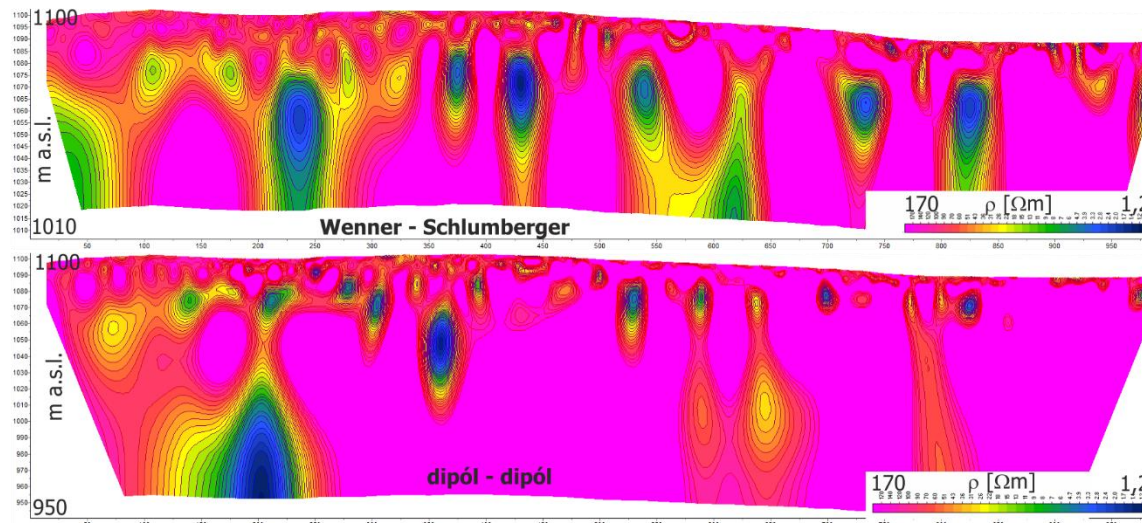


**Fig. 6** ERT in the Wenner-Schlumberger and dipole-dipole systems

individual profiles. The last question is the choice of a colour scale for the fields of resistivity values. The illustrated approach gives a possibility to perfectly describe the differences in the distribution of resistivity values on the given profile. When choosing the same colour scale for the whole site, differences between the individual profiles are easier visible and, therefore, it is possible to evaluate the whole site better. The answers to all the three questions are not easy and supporters of different solutions are found among geophysicists as well as engineering-geologists.

Of seismic measurements, we used shallow seismic refraction (SSR) and ground-based seismic tomography ST. Measurement was performed using the apparatus ELLISS-2, points of excitation of seismic energy were spaced 20 m apart in SSR and 4 m apart in ST. In both the methods, the most remote blow was 20 m behind the last geophone. 20 Hz geophones were always used always two metres apart in both the methods. Two remarks can be made to the depicted results (Fig. 7). The first is the depth depiction of the results of refraction measurements. The measurement as it was carried out brings data on the distribution of the velocities of longitudinal waves to roughly the same altitudes, not to the real depth of measurement. The depiction of the results as it is given in the figures offers the creation of assumptions that the depth of down to 28 metres was reached on profile P2 during measurement. On the opposite side, the depths are given substantially lower, namely only 17 m. On profile P1, these differences are still more significant, namely 44 m in contrast to 13 m. It would thus be more suitable to depict the field of the velocities to the assumed depth of measurement and not to terminate them at a certain altitude. This is probably an error of the program which evaluates the

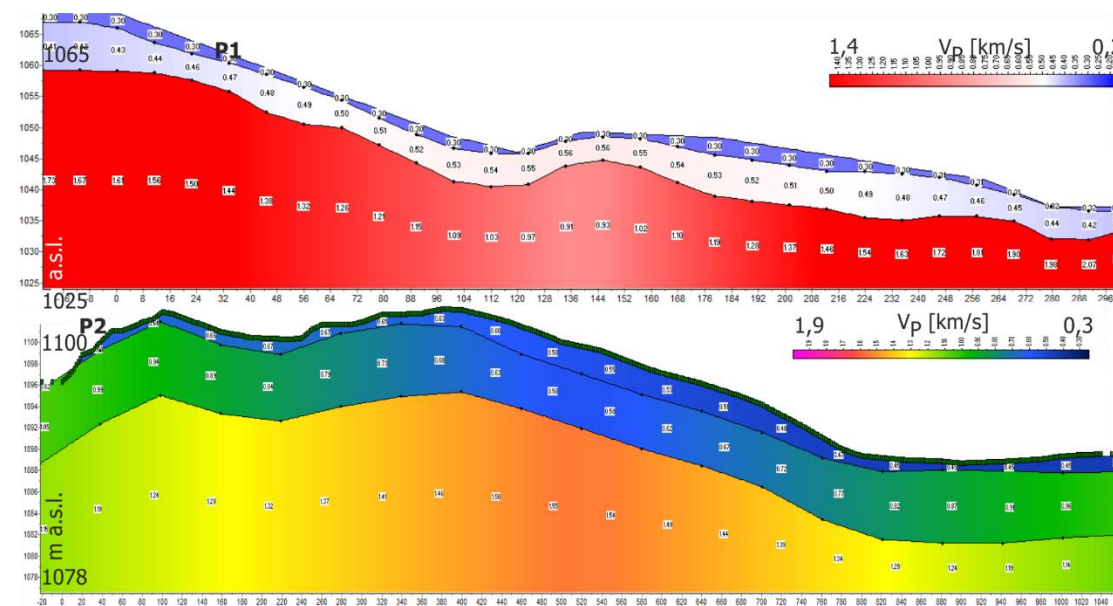


**Fig. 7** Original interpretation of shallow seismic refraction

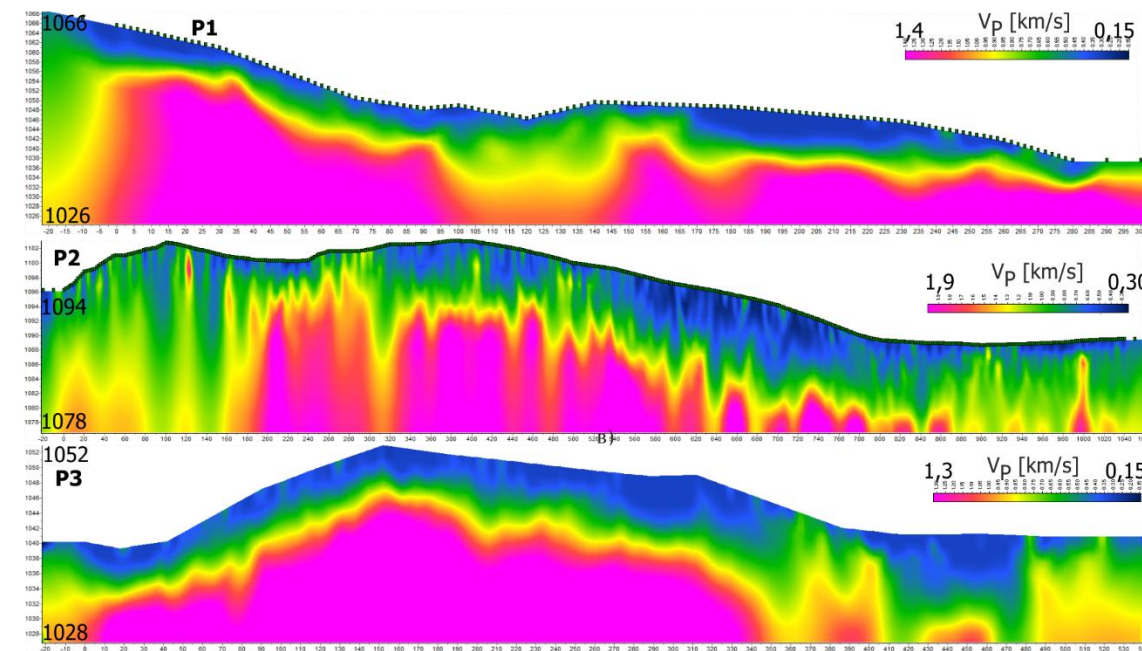


**Fig. 8** Original interpretation of ground-based seismic tomography

measurement. Another figure brings a comparison of the results of ground-based seismic tomography (Fig. 8). Here, the same remarks apply as were expressed in the description of shallow seismic refraction.

## 4. Combined geological-geophysical interpretation

### 4.1 Profiling measurements

Of the real profiling measurements, only thermometric measurement was carried out on the Staraya Podstanciya landslide. The today's system of measurement of electrical resistivity tomography and shallow seismic refraction also enables profiling curves to be obtained from them. This means for curves of apparent resistivity obtained from ERT to reorganise the output set from the apparatus Terrameter LS so that it would be possible from its part to gain changes in apparent resistivity values at selected depths for the given AB/2. The original set is organised so that it would be possible to use it for interpretation programs of ERT.

The results of profiling measurements on profile P1 are given in Figure 9. The curves of apparent resistivity indicate one anomalous place at 290 to 390 m. This, however, applies to two shorter arrays; for A10M10N40B array, the changes in apparent resistivity are minimal. It thus can be assumed that this concerns changes in the landslide (see Fig. 3). It is about a part of the landslide, which lies just below profile P3. On profile P3, it is possible to find a similar anomaly under the stations of 200 to 300 m. It is practically certain that this concerns the same anomaly which lies on the south-eastern side of a local ridge stretching in the NE–SW direction. The place of increased  $\rho_a$  in this area is marked in green in Figure 3. It is impossible to explain the geological significance in more detail from geophysical measurements. For its explanation it is necessary to make a joint inspection of an engineering geologist and a geophysicist in the field. The thermic curve was already evaluated in the preceding text; its changes have no response in the results of any other profiling measurements. The changes in the velocities in all three identified layers are gradual and do not indicate the existence of any other anomaly.

The results of measurement on profile P2 are given in Figure 10. The curves of apparent resistivity divide profile P2 into two parts. In the

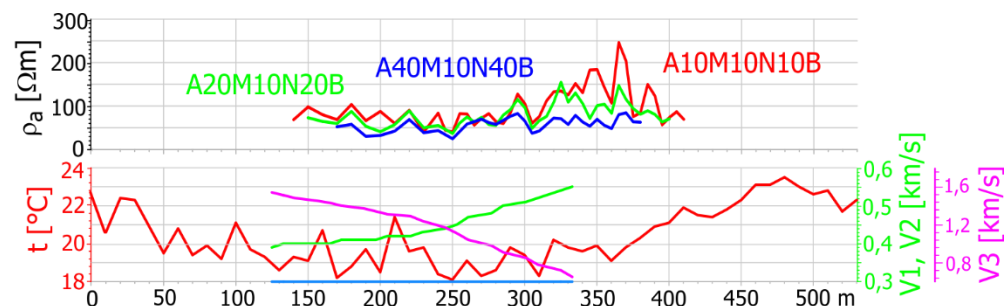


Fig. 9 Results of profiling methods on profile P1

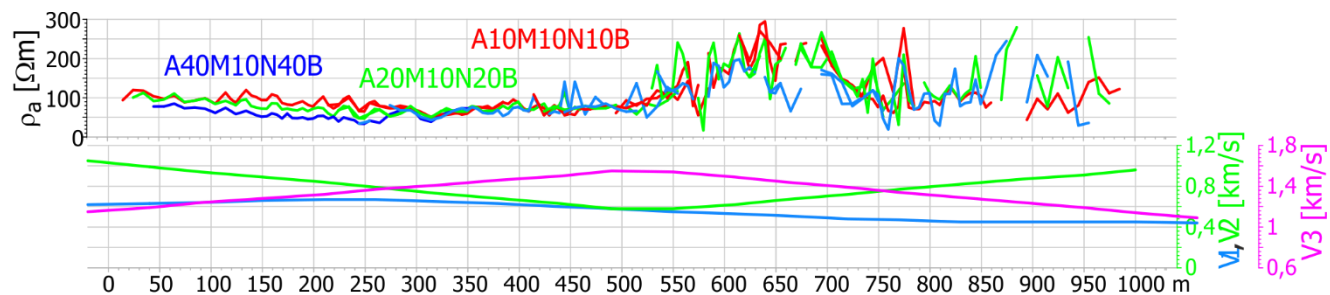


Fig. 10 Profiling measurement on profile P2

first part from the beginning of the profile to the station of about 500 m, all three curves are without substantial changes, with their values fluctuating between 40 and 100  $\Omega\text{m}$ . From 500 m to the station of 750 m, apparent resistivity values increase and are fairly variable. This applies to all three spacings as well as to the values of apparent resistivity values. In our opinion, it is necessary to look for an explanation in the distribution of mechanical stress. According to geodetic measurements, the direction of the slope failure movement is from NE to SW. Therefore, it is justifiable to believe that in this case there is an increase in tensile stress in the scarp area. This results in the formation of a larger number of open cracks and/or planes of discontinuity. From 750 metres to the end of the profile, the values  $\rho_a$  are still more fluctuating. In this case, it is possible to find more causes of this fact. The first is the increased frequency of cracks, another cause is obviously the extremely dried ground surface and the third cause is the related poor grounding of electrodes.

Thermic measurement on this profile was not carried out. Shallow seismic refraction again shows gradual changes, even in the places in which there are a larger number of open cracks. We believe that this fact is a sign of the insufficient work of the software used. It probably determines the velocities in the places of “explosion” and calculates the other velocities using the weighted average from two nearest points of explosion. This is also evidenced by the results of ground-based seismic tomography. In the field of the velocities determined by this method, the fluctuation of velocities and the existence of narrow zones with the higher or lower velocity of longitudinal waves are clearly visible (see Fig. 8).

## 4.2 Geophysical measurements behind the landslide scarp edge

One of the most important tasks in the survey of landslide places is to identify the areas from which the landslide can be recharged by groundwater. To solve this task, we used the engineering-geological mapping of the area above the slope failure and all the results of geophysical measurement available. This included archival geophysical measurement conducted in 2015 for

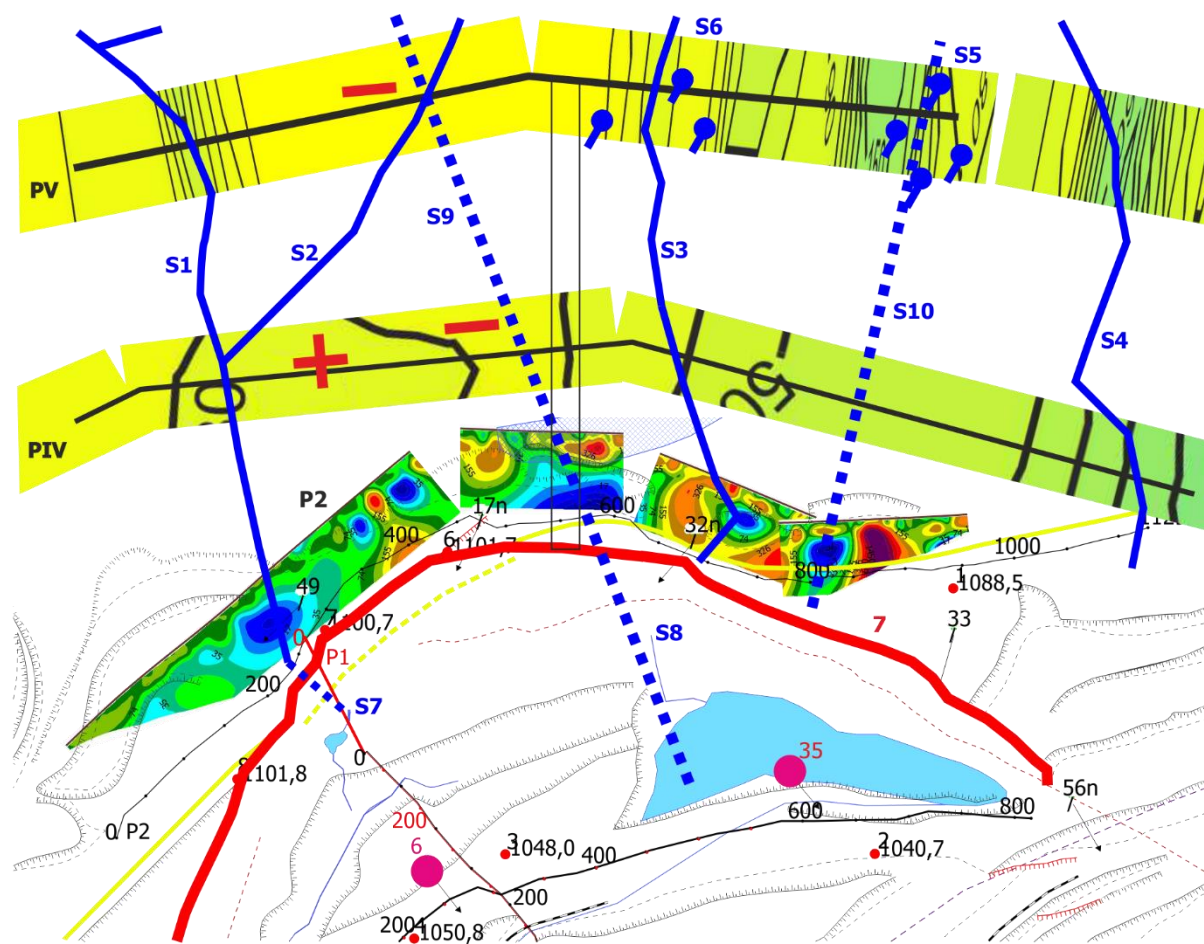


Fig. 11 Geophysical measurement behind the scarp edge



the hydrogeological survey of the area and the new measurement carried out in 2019, the task of which was to obtain information on the slope failure proper. In particular, this comprised profiles PIV and PV from 2015 and profile P2 from 2019. The result of these analyses is in Figure 11. The essential new finding was the detection of one more tectonic fracture, along which the slope failure is recharged by groundwater. The hydrogeological mapping initially discovered four positions of an intermittent surface stream, wadis S1 to S4. Some of these streams have also their subsurface cause according to the results of geophysical measurements. It is possible to clearly declare that wadi S1 can be well identified in the results of ERT obtained by interpretation using the Res2DInv program. On profile P2, a marked anomaly is visible with a decrease of resistivity below  $17 \Omega\text{m}$  under the stations of 220 to 270 m. A clear proof this fracture is the outflow of groundwater in the scarp wall of the landslide (point S7). The second such a wadi is wadi S3. It is manifested on profile P2 by a decrease in resistivity again below  $17 \Omega\text{m}$  under the station of about 690 m. This position is matched by a group of springs S6 in the upper part of the landslide. Wadi S4 could not be geophysically proved because it lies outside the range of geoelectrical measurements. The geoelectrical anomaly of the minimum at 820 m (less than  $17 \Omega\text{m}$ ) was not mapped on the ground surface, but it can correspond to a group of springs S5; in this case, it thus concerns fracture S10. Another line which provably recharges the landslide by groundwater is line S9. It is manifested on P2 by the most striking resistivity anomaly from 520 to 610 m with a resistivity value below  $8 \Omega\text{m}$ . On profile PIV, it is shown by a resistivity minimum on the contours of apparent resistivity obtained from VES (in deep yellow colour). The same applies to profile PV, on which it crosses wadi S2. This line, in all likelihood, most strongly recharges the slope failure by groundwater. This claim is also evidenced by the largest lake on the landslide, which never dries out according to satellite images. The other wadis often lay in local resistivity maxima at the time of measurement, which can signify that the given tectonic fracture was not water-bearing at the time of measurement.

### 4.3 Comprehensive interpretation of profile P1

The last step of the overall processing of geophysical measurements lasting many years on the Staraya Podstanciya landslide failure was a comprehensive evaluation of such measurements on profile P1. On this profile, the results of measurement of the Uzbek party were available, namely thermic profiling, electrical resistivity tomography, shallow seismic refraction and ground-based seismic tomography. Within the overall interpretation, graphs of changes in the velocities of longitudinal waves V1, V2 and V3 were constructed from shallow seismic refraction. As already mentioned in the preceding text, the program used does not evaluate field measurement in sufficient detail. The program strongly generalises the changes in velocities, and thus the graphs of changes in the velocities of longitudinal

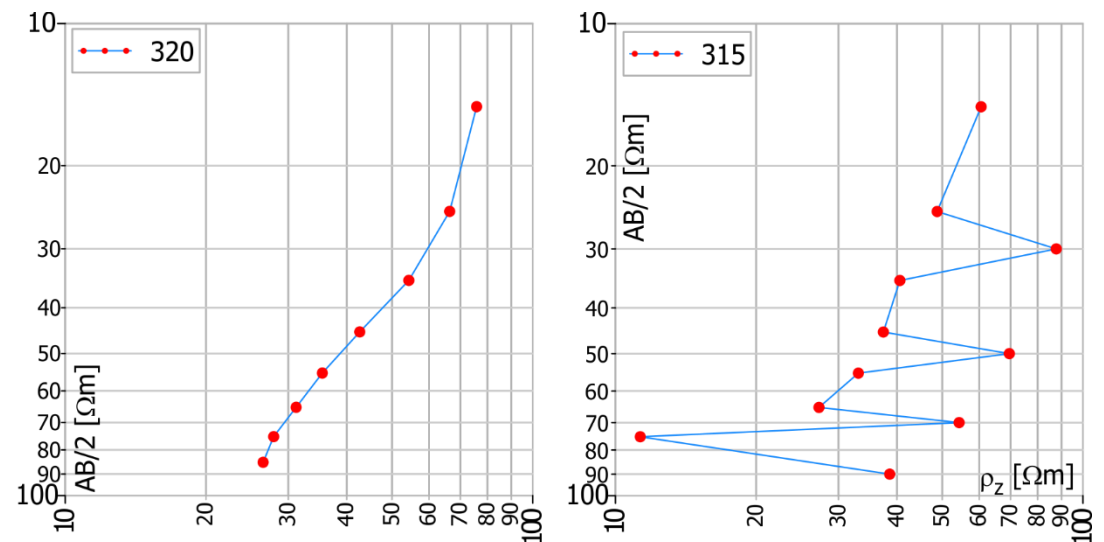
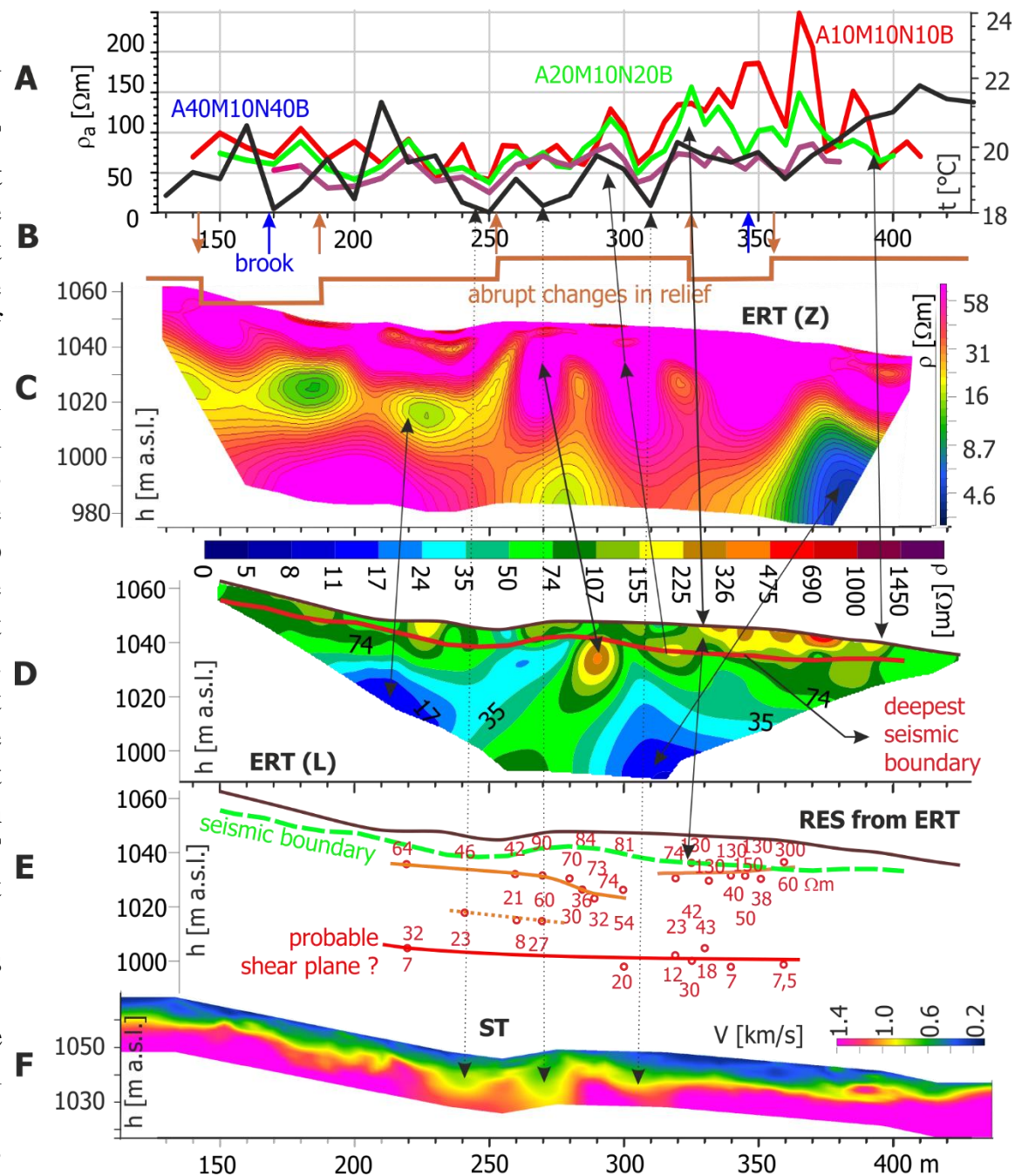


Fig. 12 Curves of RES obtained from ERT measurement

waves were excluded from further processing. In addition, graphs of changes in apparent resistivity were constructed along the profile for spacings of A10M10N10B, A20M10N20B and A40M10N40B obtained from ERT measurement. The spacings were chosen so that they can best describe changes inside the rock mass. Deeper spacings were not monitored because the system of ERT measurement at greater depths does not monitor the given profile in its whole length any more. Another step was to construct the curves of vertical resistivity sounding obtained from ERT measurement. The curves of VES can be constructed in such a case in a 150-m-long inner section of the profile, i.e. in a part of about 40% of the length of the electrode array. This system of VES processing results from research work of the company Geotest (Bláha et al., 2021). Figure 12 depicts two such obtained VES as an example. One good curve and one curve with incorrect values are shown quite deliberately. It becomes evident that not all measurements in ERT are correct. The system of internal control of the program of measurement obviously does not exclude poorly grounded electrodes and the program of inversion probably does not eliminate all incorrect values of measured resistivity. It is natural that this fact is then depicted in the resulting resistivity field obtained from ERT measurement. In this evaluation it is necessary to realise that measurement in the field took place in very difficult conditions. The very disturbed topography of the slope, frequent cracks (mostly open), the dried ground surface and, conversely, muddy terrain in some places do not certainly increase the quality of measurement. Nevertheless, the data obtained from VES provided material suitable for further investigation.

Figure 13 shows six partial graphs depicting the results of individual methods. Graph A refers to profiling thermic and



**Fig. 13 Comprehensive profile interpretation P1**

resistivity methods. These results were already described in the preceding chapters. Graph B illustrates prominent benches of the topography of terrain and the existence of water streams on the profile. This graph was constructed as an aid for evaluating the other methods.

Graph C shows the results of electrical resistivity tomography interpreted by the ZondRes2D program. In the ERT cross-section, in relation to resistivity, the occurrence of a low-resistivity layer is relatively clearly indicated in the central part of the section, being 15–22 m thick, which is found in the upper part of the profile at depths of about 17–25 m. In the central part of the profile, it submerges to depths of about 46–48 m. Under the stations of 240–280 m, an anomalous low-resistivity zone was revealed, being 30–35 m thick. This all indicates the occurrence of preferred pathways of groundwater in this section. Groundwater is accumulated in the lower part of the section. The decrease of resistivity is also influenced by the fracturing of chiefly clayey rocks. When fractured and water saturated, their resistivity can decrease even below 10  $\Omega\text{m}$ .

Graph D depicts the results of inversion of Uzbek measurements obtained using the Res2DInv program. Perhaps the greatest difference, even though formal in a certain sense of the word, is the areal size of depicted resistivity fields. The ZondRes2D program illustrates the results relatively far behind the measured end points. A certain insufficiency of this graph is the different scale of resistivity values of both resistivity fields. This was caused by rapid adding the Czech interpretation to the original Uzbek results. The field of these resistivity values depicts the deepest seismic boundary as shown by the SSR method. It becomes evident that this boundary corresponds well to the surface layer of higher resistivity values, which was detected by both methods of inversion. This increase of resistivity values is also visible on the curves of resistivity profiling under the stations of 315–390 m. Interesting is the position of higher resistivity values on ERT (L) under the station of 290 m. This also matches the increased resistivity values on ERT inversion (Z). Both of these anomalies in the figure are connected by a line with arrows. A resistivity maximum on ERT (L) at 32 metres is reflected on the resistivity profiling of particularly shallow and medium spacing of around 295 m. Resistivity minima of ERT also correspond well with one another in both of the methods of inversion under the station of 220 m. Somewhat worse is the agreement of the second resistivity minima under the station of 310 and 380 m, respectively. The explanation must be searched in the capabilities of 2D measurement and 2D processing. These do not assume the oblique angle of inhomogeneities in relation to the measured profile. The mathematical method of searching the best solution can be carried out in different ways.

Graph E shows the results of conventional interpretation of vertical electrical sounding. How the conditions of measurements were complicated is also evident from the determination of depths and resistivity values of individual boundaries. Even though some VES points were five metres apart from one another, yet identical results were not detected in two neighbouring points practically in any case. Also for this reason, the rule that the boundary must be drawn through the interpreted depth was not followed in determining the boundaries of individual media. The boundaries were determined in an effort to keep a certain continuity of the geological boundary. The plotted deepest seismic boundary in a section between 315 m and the end of the profile corresponds well with the base of higher resistivity values of both ERT interpretations. According to the results of VES, the resistivity values rise up to 300  $\Omega\text{m}$  in this layer. This can signify the occurrence of sands or gravels which are mentioned in the geological description of the site. The second geoelectrical boundary at 220 to 300 m is probably the boundary between different Quaternary soils, which could obviously be more clayey at their base. The deepest boundary running

along the whole section, in which it was possible to interpret VES, is, in all likelihood, the Quaternary/Neogene boundary. There will always be a possibility that certain movements could take place along this boundary inside the slope failure.

The lowest graph shows the results of ground-based seismic tomography. The program for its processing works indisputably better than the program for processing shallow refraction sounding. The most interesting changes were identified under the stations of 230 to 280 m, i.e. in the places in which terrain slightly rises into the opposite slope. This whole section is bound by two zones of drop of velocities down to 1.0 km/s to the depths of 27 and 37 m, respectively. It is interesting that these zones lie close to a terrain bench under the station of 260 m. In most likelihood, some physical or geological cause of this feature must exist, but a more detailed explanation would require a field visit of the site. Both of the zones of minima of velocities in this place are manifested on thermic measurements by a drop of temperature down to 18°C. A similar zone, though not so significant in terms of velocity, lies under the station of 305 m. All of the three zones are interconnected with a dotted line in Figure 12. Also in this case, we could not find a physical or geological cause of this feature.

The last figure depicts the results of interpretation of geophysical measurement projected into the original engineering-geological cross-section (Fig. 14). Unfortunately, in this comparison, the precise location of the geological cross-section relative to the geophysical profile was not available to us. When projecting the results of geophysics into the geological cross-section, we followed the rule to keep the same altitudes. The lines of the altitude 1060 m were laid on top of one another in both of the cross-sections. Side alignment resulted from the fact that zero of geophysical measurements had been on the scarp edge of the slope failure. In the end part of the geophysical profile, a significant drop of the ground surface took place over the last year. The shallowest geophysically identified boundaries correspond to the different boundaries of Quaternary soils. The lowest physical boundary corresponds to the contact between Neogene and Quaternary sediments.

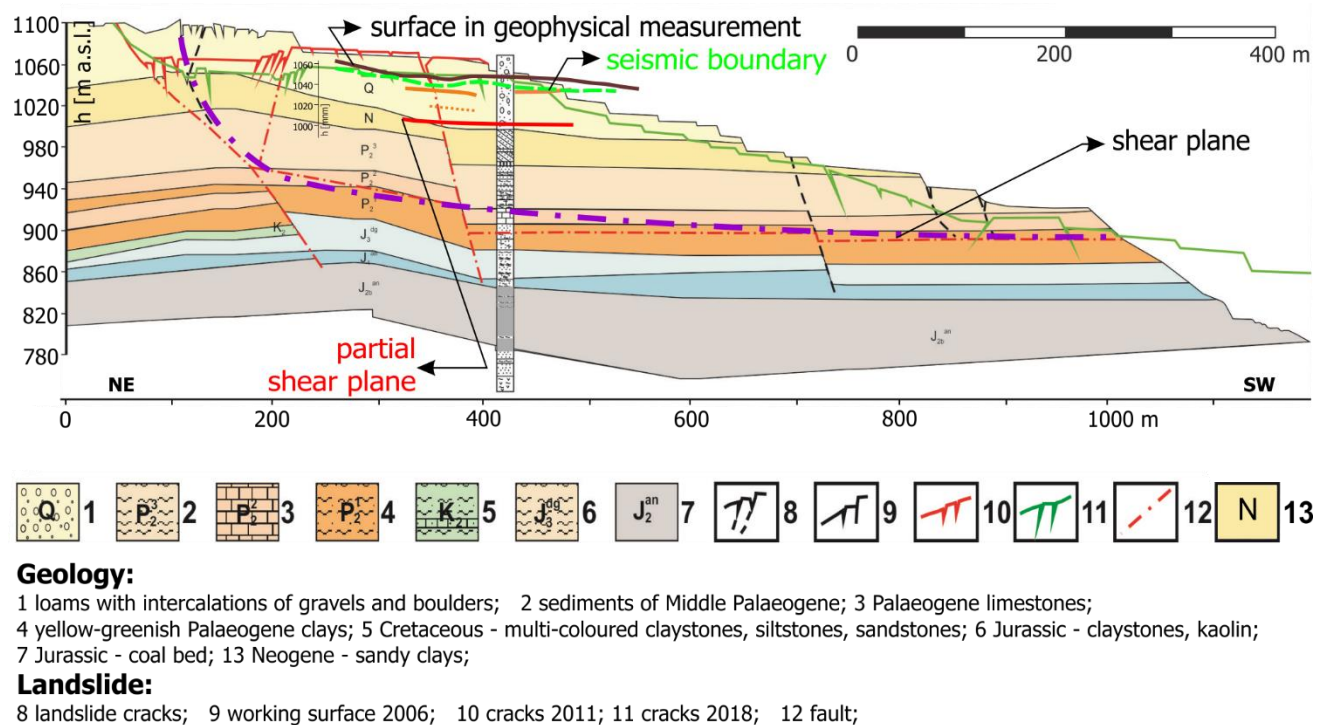


**Fig. 14 Engineering-geological cross-section through the landslide**

## 5. Conclusion

This paper deals with the use of geophysical measurements during the research of slope failures. It concerns the Staraya Podstanciya landslide, which is an extensive landslide on the wall of a coal pit, where the velocity of movement reached up to 750 mm per day. Geophysical measurement included measurement conducted in the years 2015 and 2019, particularly thermic profiling, electrical resistivity tomography, vertical electrical sounding, shallow seismic refraction and ground-based seismic tomography. Within processing, curves of resistivity profiling were constructed from ERT measurement, as well as curves of vertical electrical sounding. Velocities of longitudinal waves on three refractive interfaces were compiled from shallow seismic refraction. It was detected that such obtained curves of seismic profiling had not brought the expected benefit. The reason is the interpretation program which smooths the real changes of velocities too much on all refraction horizons. Res2DInv and ZondRes2D programs were used for the interpretation of ERT measurements.

Of profile measurements, the greatest benefit was brought by measurement of resistivity profiling. This reveals the values of increased apparent resistivity, which were subsequently evaluated as the zones of increased mechanical stress and the zones of significantly increased cracking. In addition, resistivity profiling showed an area of increased apparent resistivity values in the middle of the slope failure. This place is probably formed by more sandy soils with a possible admixture of gravels. This islet can recharge the slope failure by water which flows down the surface in case of clayey soils, but in this case it infiltrates into the body of the landslide. Thermic measurements revealed places with a changed temperature, but we could not find a clue how to interpret such places geologically. In relation to the above mentioned, seismic profiling was excluded from further processing.

As the greatest benefit of the comprehensive processing of geophysical measurements, we can consider the identification of two zones through which the landslide is recharged by groundwater from the higher lying rock mass; it subsequently decreases the level of the landslide stability. The Czech authors are of such an opinion that greater attention should be given to pumping water from lakes on the landslide. This discovery has shown how important is to use also measurements carried out before starting the current project for the solution of the chosen problem. Important information can also be obtained from measurements which were carried out using a system other than that enabled by the current technology of geophysical measurement and data processing.

The last example of the results of interpretation of old as well as new measurements and the use of different programs for measurement processing is in the last figure of this paper. It shows the results of measurement and interpretation on profile P1. The figure presents six different outputs, from which are subsequently derived the discoveries that indicate the geological conditions of the investigated area. The most substantial discoveries were the identification of places in which the slope failure is recharged by water from higher lying places and in which infiltration of precipitation water into the landslide can be more significant. Sounding measurements have shown a possible partial shear plane at the boundary between Quaternary and Neogene sediments. In addition, geophysical measurement was successful in locating places with increased tensile stress and places of a significant increase of cracking of the rock mass.

## References

- ABDULLAEV, SH. KH., MOTORNY, I.R., RASULEV, B.B. Zpráva na téma č. 435 "Zkvalitnění geofyzikálního průzkumu za účelem zvýšení hloubky, detailnosti a spolehlivosti při řešení inženýrsko-geologických a hydrogeologických problémů." (Report on theme no. 435 "Improvement of a geophysical survey to increase depth, detail and reliability in solving engineering-geological and hydrogeological problems"), Fondy státní instituce „GIDROINGEO Institute“ (Funds of the state-owned "GIDROINGEO Institute"), Tashkent, 2020, 187 p.
- BLÁHA, P. *Ověřená technologie, Rozvoj geotechnických a geofyzikálních metod pro získání 2D a 3D obrazu geologické stavby (Verified technology, Development of geotechnical and geophysical methods to obtain 2D and 3D images of the geological structure)*, GEOTest a.s., 2021, 80 p.
- BLÁHA, P., DURAS, R., GEBAUER, J., STAŠ, L., WACLAWIK, P., KRÁLOVCOVÁ, J., BŘEZINA, J., SRB, R. *FV20294 Rozvoj geotechnických a geofyzikálních metod pro získání 2D a 3D obrazu geologické stavby (Development of geotechnical and geophysical methods to obtain 2D and 3D images of the geological structure)*, Závěrečná zpráva (Final report), GEOTest a.s., 2021, 53 p.
- NIYAZOV, R.A., ABDULLAEV, SH.KH., MOTORNY, I.R., RASULEV, B.B. *Zpráva na téma č. 448 „Posouzení náchylnosti k rezonančním oscilacím sesuvů v Uzbekistánu“*, (Report on theme no. 448 "Assessment of susceptibility to resonant oscillations of landslides in Uzbekistan"), Fondy státní instituce „GIDROINGEO Institute“ (Funds of the state-owned "GIDROINGEO Institute"), Tashkent, 2020, 58 p.
- TÁBOŘÍK, P., GEBAUER, J., DURAS, R., BLÁHA, P. The mystique of ERT. *EGRSE*, XXIV.2, ČAAG, 2017/2, ISSN 1803–1447, pp. 28-37.

---

### Authors:

<sup>1</sup> doc. RNDr. Pavel Bláha, DrSc., GEOTest, a.s., Švehlova 26, Praha 10, 106 00, Czech Republic, [blaha@geotest.cz](mailto:blaha@geotest.cz)

<sup>2</sup> Ing. Shavkat Abdullaev, CSc., Institute of Hydroingeo SE, 64, Olimlar Str, Tashkent City 100041, Uzbekistan, [abdullaevs@mail.ru](mailto:abdullaevs@mail.ru)

<sup>2</sup> Mgr. Igor Motornij, Institute of Hydroingeo SE, 64, Olimlar Str, Tashkent City 100041, Uzbekistan, [imotornij2014@gmail.com](mailto:imotornij2014@gmail.com)

<sup>2</sup> Ing. Rustam Niyazov, CSc., Institute of Hydroingeo SE, 64, Olimlar Str, Tashkent City 100041, Uzbekistan

<sup>1</sup> Ing. Jan Gebauer, GEOTest, a.s., Kapitální 13, Ostrava, 700 30, Czech Republic, [gebauer@geotest.cz](mailto:gebauer@geotest.cz)

<sup>3</sup> Ing. Milan Lazecký, PhD., School of Earth and Environment University of Leeds, Woodhouse Ln LS2 9JT, Leeds, United Kingdom, [M.Lazecky@leeds.ac.uk](mailto:M.Lazecky@leeds.ac.uk)